Looking at Friction through "Shearons"†

Markus Porto, Michael Urbakh, and Joseph Klafter*

School of Chemistry, Tel Aviv University, 69978 Tel Aviv, Israel

Received: December 1, 1999

We study the response to shear of a one-dimensional monolayer embedded between two rigid plates, where the upper one is externally driven. The shear is shown to excite "shearons", which are collective modes of the embedded system with well-defined spatial and temporal patterns, and which dominate the frictional properties of the driven system. We demonstrate that static friction, stick−slip events, and memory effects are well described in terms of the creation and/or annihilation of a shearon. This raises the possibility of controlling friction by modifying the excited shearon, which we exemplify by introducing a defect at the bottom plate.

The field of nanotribology evolves around the attempts to understand the relationship between macroscopical frictional response and microscopic properties of sheared systems.[1,2] New experimental tools such as the surface forces apparatus (SFA) are used to explore shear forces between atomically smooth solid surfaces separated by a nanoscale molecular film.[3] These experiments have unraveled a broad range of phenomena and new behaviors which help shed light on some "old" concepts which have been considered already textbook materials: static and kinetic friction forces, transition to sliding, thinning, and memory effects. These and other observations have motivated theoretical efforts,[4−15] both numerical and analytical, but many issues remain unresolved, in particular the relation between the macroscopic observables and the microscopic properties of the embedded system.

In this Article we introduce the concept of "shearons", which are shear-induced collective modes excited in the embedded system and characterized by their wave vector q. Shearons, which display well-defined spatial and temporal patterns, dominate the frictional properties of the driven system and are found useful in establishing a connection between frictional response and motional modes of the embedded system. Within this framework observations such as static friction, stick−slip behavior, and memory effects can be correlated with the creation and/or annihilation of a shearon. These correlations suggest the possibility of controlling friction by modifying the shearon's wave vector and thereby tuning the embedded system by adding, for example, a defect at one of the plates.

We start from a *microscopic* model which has been investigated recently and has been shown to capture many of the important experimental findings.[6,10] The model system consists of two rigid plates, with a monolayer of N particles with masses m and coordinates x_i embedded between them. The top plate with mass M and center-of-mass coordinate X is pulled with a linear spring of spring constant K. The spring is connected to a stage which moves with velocity V. This system is described by $N + 1$ equations of motion:

$$M\ddot{X} + \sum_{i=1}^{N} \eta[\dot{X} - \dot{x}_i] + K[X - Vt] + \sum_{i=1}^{N} \frac{\partial \Phi(x_i - X)}{\partial X} = 0 \quad (1)$$

$$m\ddot{x}_i + \eta[2\dot{x}_i - \dot{X}] + \sum_{\substack{j=1 \\ j\neq i}}^{N} \frac{\partial \Psi(x_i - x_j)}{\partial x_j} + \frac{\partial \Phi(x_i)}{\partial x_i} + \frac{\partial \Phi(x_i - X)}{\partial x_i} = 0 \quad i = 1,...,N \quad (2)$$

The second term in eqs 1 and 2 describes the dissipative forces between the particles and the plates and is proportional to their relative velocities with proportionality constant η, accounting for dissipation that arises from interactions with phonons and/or other excitations. The interaction between the particles and the plates is represented by the periodic potential $\Phi(x) = -\Phi_0 \cos(2\pi x/b)$. Concerning the inter-particle interaction, we assume nearest-neighbor interactions of two types: (i) harmonic interaction $\Psi(x_i - x_{i\pm1}) = (k/2)[x_i - x_{i\pm1} \pm a]^2$ and (ii) Lennard−Jones interaction $\Psi(x_i - x_{i\pm1}) = (ka^2/72)\{[a/(x_i - x_{i\pm1})]^{12} - 2[a/(x_i - x_{i\pm1})]^6\}$.[16] The two plates do not interact directly.

The basic frequency is chosen to be the frequency of the top plate oscillation in the potential $\Omega \equiv (2\pi/b)\sqrt{N\Phi_0/M}$. The other frequencies in the model are the frequency of the particle oscillation in the potential $\omega \equiv (2\pi/b)\sqrt{\Phi_0/m}$, the characteristic frequency of the inter-particle interaction $\hat{\omega} \equiv \sqrt{k/m}$, and the frequency of the free oscillation of the top plate $\hat{\Omega} \equiv \sqrt{K/M}$. To simplify the discussion we introduce unitless coordinates $Y \equiv X/b$ and $y_i \equiv x_i/b$ of the top plate and the particles, respectively, as well as the unitless time $\tau \equiv \Omega t$. We define the following quantities: The misfit between the substrate and inter-particle potentials' periods $\Delta \equiv 1 - a/b$, the ratio of masses of the particles and the top plate $\epsilon \equiv Nm/M$, the unitless dissipation coefficient $\gamma \equiv N\eta/(M\Omega)$, the ratio of frequencies of free oscillation of the top plate and the oscillation of the top plate in the potential $\alpha \equiv \hat{\Omega}/\Omega$, the ratio of the frequencies related to the inter-particle and particle/plate interactions $\beta \equiv \hat{\omega}/\omega$, and the dimensionless velocity $v \equiv V/(b\Omega)$. Additionally, the friction force per particle f_k is defined as $f_k \equiv F_k/(NF_0)$,

† Part of the special issue "Harvey Scher Festschrift".

* Author to whom correspondence should be addressed.

10.1021/jp994285h CCC: $19.00 © 2000 American Chemical Society
Published on Web 04/05/2000

where F_k is the total friction force measured with the external spring and $F_0 \equiv 2\pi\Phi_0/b$ is the force unit given by the plate potential. Here, we keep fixed the number of particles $N = 15$, the mass ratio $\epsilon = 0.01$, the misfit $\Delta = 0.1$, and the relative strength of the inter-particle interaction $\beta^2 = 1$. We vary only the relative strength of the external spring α^2, the dissipation coefficient γ, and stage velocity v.

In order to analyze the motion of the embedded system more closely, we separate the motion of the particles into the center of mass part $y_{cms} \equiv 1/N \sum_{i=1}^{N} y_i$ and the fluctuations $\delta y_i \equiv y_i - y_{cms}$.[17] It has been observed in similar models[18−20] that different modes of motion can coexist for a given set of parameters and lead to different frictional forces. Here, we concentrate on these solutions of the coupled dynamical eqs 1 and 2 which correspond to smooth or to stick−slip motion of the top plate. To understand the nature of the motion of the embedded system in these regimes and the relation to the frictional response, we choose the particles' density ρ as a observable. Instead of defining the density as $\sum_{i=1}^{N} \delta(y - y_{cms} - \delta y_i)$, we represent each particle by a Gaussian of width $\sigma = 1$, namely,

$$\rho(y - y_{cms}, \tau) \equiv \sum_{i=1}^{N} \exp\left\{-\left[\frac{y - y_{cms} - \delta y_i}{\sigma}\right]^2\right\} \qquad (3)$$

This allows us to visualize correlated motions of the particles on length scales which exceed nearest-neighbor distance and are of the order of 2σ to 3σ. Using eq 3 we find that the response of the embedded system to shear can be described in terms of collective modes which result in well-defined spatial and temporal pattern in the density, which we call "shearons". These shearons are the spatial/temporal manifestation of parametric resonance between the external drive and the embedded system,[20,21] and are characterized by their wave vector q (see Figure 1a−c).

In Figure 1a−c we present three *stable* shearons for a chain of harmonically interacting particles with free boundary conditions, where in all cases the top plate slides smoothly. All three shearons share the same set of parameters and differ only in their initial conditions. We find that the observed mean friction force per particle $\langle f_k \rangle$ ($\langle \cdot \rangle$ denotes time average), which is directly related to the spatial/temporal fluctuations[21]

$$\langle f_k \rangle = \pi\gamma v + \frac{2\pi\gamma}{v} \langle \sum_{i=1}^{N} \delta \dot{y}_i^2 \rangle \qquad (4)$$

decreases with increasing shearon wave vector q for fixed stage velocity v, i.e., $(\partial\langle f_k \rangle/\partial q)_v < 0$. This means that the mean friction force can be reduced by increasing the shearon wave vector (see below for possible methods). In the present example, we observe a reduction from $\langle f_k \rangle \cong 0.263$ (Figure 1a) to $\langle f_k \rangle \cong 0.180$ (Figure 1b), and to $\langle f_k \rangle \cong 0.125$ (Figure 1c). The lowest possible mean friction force $\langle f_k \rangle = \pi\gamma v$ can be achieved in the limit $q \to \infty$. For our choice of parameters $\pi\gamma v \cong 0.04712$.

We find that the regions of high density fluctuations exhibit low velocity fluctuations and, according to eq 4, low dissipation. These regions are surrounded and stabilized by regions of low density fluctuations with highly fluctuating velocities and hence high dissipation. We note that the minima/maxima of the density reflect correlations in the motion of the neighboring and next-neighboring particles rather than actual locations. The cooperative nature of motion is visualized here introducing a finite width σ.

As we have already seen, larger wave vectors correspond to higher average density of the embedded system. This means

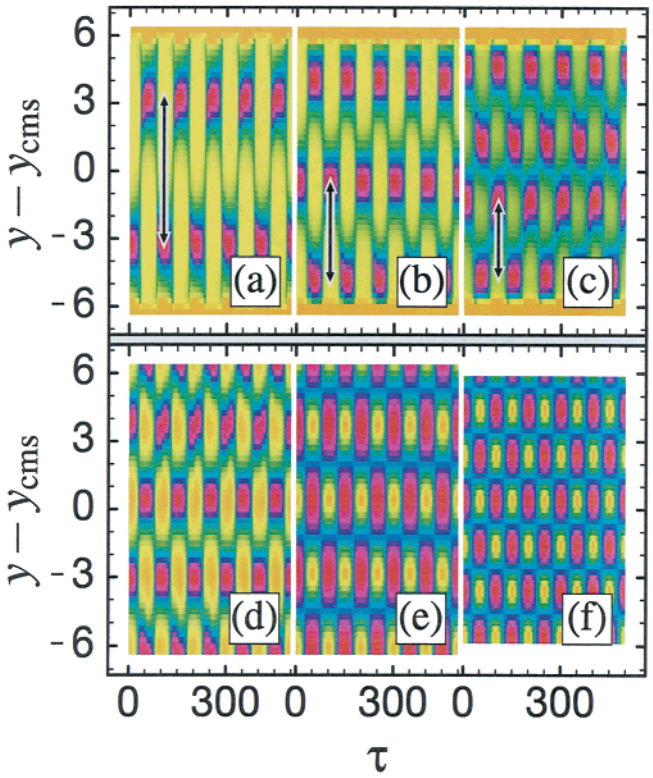

Figure 1. Plot of the particles density ρ vs position $y - y_{cms}$ and time τ for different shearons. The orange, yellow, green, blue, and red colors indicate increasing density (the color scales are chosen independently for each subfigure to maximize contrast). In (a)−(c), three different stable shearons are shown for a chain with free ends. In (d)−(f) periodic boundary conditions are used with box sizes $l = 13$, 13, and 12. Harmonic interaction between the particle is assumed in (a)−(d) and Lennard−Jones interaction in (e) and (f). The arrows shown in (a)−(c) indicate the respective $1/(2q)$. The resulting mean friction forces in (a)−(f) are $\langle f_k \rangle \cong 0.263$, 0.180, 0.125, 0.123, 0.060, and 0.047. The model parameters are $\alpha = 1$, $\beta = 1$, $\gamma = 0.75$, $\Delta = 0.1$, $\epsilon = 0.01$, $N = 15$, and $v = 0.02$.

that for a given number of particles the mean chain length $\langle L \rangle \equiv \langle y_N - y_1 \rangle$ decreases with q: $\langle L \rangle \cong 13$ (Figure 1a), $\langle L \rangle \cong 12.5$ (Figure 1b), and $\langle L \rangle \cong 12$ (Figure 1c). Note that for $N = 15$ and $\Delta = 0.1$ the equilibrium length of the free chain is 12.6. The interplay between mean length $\langle L \rangle$ and the shearon wave vector q becomes clearer within the calculations under periodic boundary conditions, where q is a function of the box size l (see Figure 1d−f). In Figure 1d we present the spatial/temporal pattern found for harmonically interacting particles within a box of size $l = 13$. It is found that for similar wave vectors the mean friction force is smaller for the case of periodic boundary conditions compared to a free chain (cf. Figure 1c), since the free ends strongly fluctuate and cause additional dissipation.

When replacing the harmonic with the Lennard−Jones interaction (see Figure 1e, f), the picture remains basically unchanged. The essential differences are found for (i) very large box sizes, when the embedded Lennard−Jones system breaks and one reobtains the independent particle scenario described in ref 6; and (ii) very small box sizes, when the hardcore of Lennard−Jones potential becomes dominant. The latter case corresponds to the high pressure limit $p \propto l^{-1} \to \infty$ and results in a strong stiffness. This, together with incommensurability, allows us to achieve the lower bound for the mean friction force $\langle f_k \rangle = \pi\gamma v$, cf. eq 4. In the case of harmonically interacting particles, minima of the mean friction force $\langle f_k \rangle$ as a function of box size l are found for finite values of l, which are

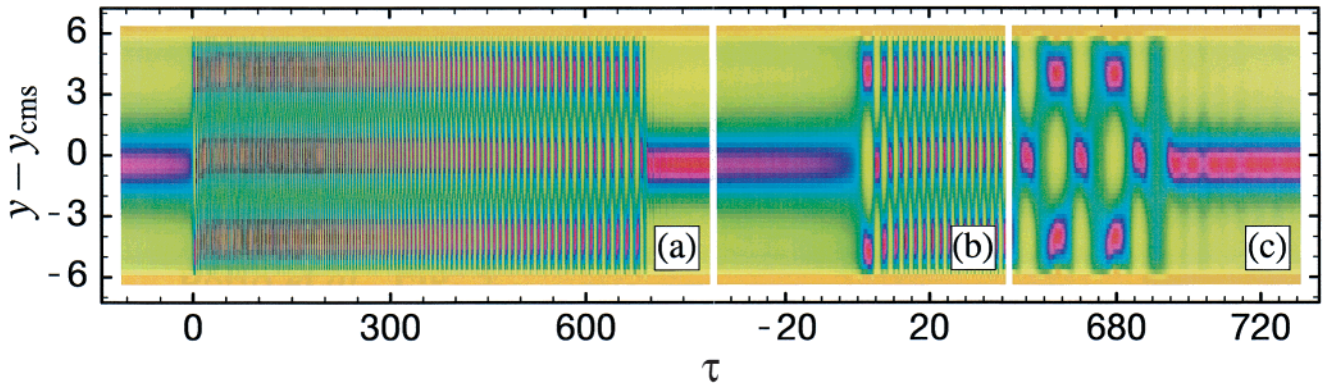

Figure 2. Plot of the particles' density ρ vs position $y - y_{cms}$ and time τ for parameters that correspond to periodic stick−slip motion. In (a) we focus on the time interval of a single slip event. The slip starts at $\tau \cong 0$ (largest spring force) and persists until $\tau \cong 689$ (smallest spring force), (b) and (c) show enlargements of the regions where the motion of the top plate starts and stops. The model parameters are $\alpha = 0.02$, $\beta = 1$, $\gamma = 0.1$, $\Delta = 0.1$, $\epsilon = 0.01$, $N = 15$ (harmonic interaction and free boundary conditions), and $v = 0.06$.

determined by commensurate condition of shearon wave vector and the box size. These effects will be discussed elsewhere.[22]

We now explore the concept of shearons in relationship to various frictional phenomena. We start from the well-known stick−slip phenomenon observed in many nanoscale systems at low driving velocity, but whose nature is still not well understood. The start of a slip event has been commonly attributed to the "melting" of the embedded system, namely a transition from a ordered "solid"-like to a disordered "liquid"-like structure, that "refreezes" at the end of the slip event. In Figure 2a we show that during slippage the motion of the embedded system is *highly ordered* and *highly correlated.* At the start of the slip event, the moment of the highest spring force (enlarged in Figure 2b), a shearon is created, persisting with a constant wave vector until it gets annihilated at the moment of the lowest spring force (enlarged in Figure 2c). The shearon gets annihilated since it cannot exist below a certain shear force needed to compensate the energy dissipation. As a result we find that the static force f_s needed to be overcome in order to initiate the motion is the shear force needed to create the shearon. This becomes clearer in a stop/start experiment, where for a smoothly sliding top plate the external drive is stopped for a certain time and reinitiated afterwards. We find that the static friction force needed to restart the motion manifests a stepwise behavior as a function of stopping time.[23] It vanishes only as long as the motion is restarted within the lifetime of the shearon, giving a possible explanation of the memory effects observed in ref 24.

Since within the shearon description the frictional force is determined by the wave vector, it is suggestive to influence the friction by modifying q. It is possible to change the shearon wave vector by changing external parameters such as the stage velocity (a higher velocity results in general in a larger wave vector). A shearon with a large wave vector, created at a high velocity, can be maintained at lower velocities by deceleration, giving rise to a hysteretic behavior observed in many experimental systems.[3]

Here, we present as an example a "chemical" method to manipulate the shearon wave vector by introducing a defect. The defect is placed at the bottom plate at an integer position y_0, leading to a modified bottom plate potential $\Phi'_{y_0}(y) = \Phi_0(1 - h\{1 + \cos(2\pi[y - y_0])\})$ for $|y - y_0| \leq 1/2$ and $\Phi'_{y_0}(y) = \Phi(y)$ otherwise. Here h defines the relative depth of the minimum at position y_0, with $h = 1$ being the regular case. As an example, the resulting density pattern for $h = 0.5$ is shown in Figure 3, where it can be seen that scattering by the defect changes the shearon wave vector q into a new wave vector q'

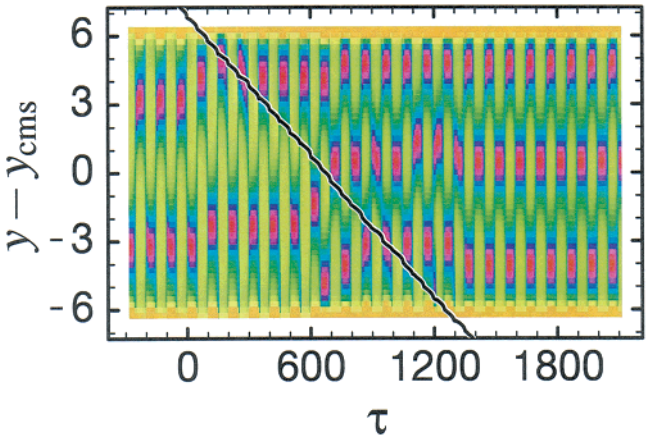

Figure 3. Modifying a shearon by a defect; plotted is the particles' density ρ vs position $y - y_{cms}$ and time τ. The shallow defect is reached by the first particle at $\tau \cong 0$ and left by the last particle at $\tau \cong 1346$. The relative position of the defect is shown as a black line. The scattering by the defect increases the shearon wave vector, which results in a decrease of the mean friction force from $\langle f_k \rangle \cong 0.263$ to $\langle f_k \rangle' \cong 0.178$. The model parameters are $\alpha = 1$, $\beta = 1$, $\gamma = 0.75$, $\Delta = 0.1$, $\epsilon = 0.01$, $N = 15$ (harmonic interaction and free boundary conditions), $v = 0.02$, and $h = 0.5$.

$> q$. The new shearon with wave vector q' is *stable*, leading to a decrease of the mean friction force from $\langle f_k \rangle \cong 0.263$ before passing the defect to $\langle f_k \rangle' \cong 0.178$ afterwards. Depending on the amplitude of h, both a decrease and an increase of the friction force are possible, which provides a method to tune $\langle f_k \rangle$. It was already observed in similar models that disorder can significantly change the frictional behavior.[13,19]

In this Article we have introduced the concept of shearons, which are shear-induced collective modes in the embedded system, and have demonstrated that their properties dominate the frictional behavior of the driven system. Furthermore, we have established a relationship between the macroscopic frictional behavior of the system and the microscopic modes of motion. The results have been obtained for a certain set of parameters describing the embedded system. However, the collective effects discussed above have a general nature and have been found in a wide range of parameters, except for the limits $N \to 1$, $\beta \to 0$, and/or $\Delta \to 0$, which correspond to the case of independent particle motion. We believe that the observed collective modes of motion are even more general and should not depend on the one-dimensionality of our model. In particular, we expect shearons to persist in systems of higher dimension, as long as the embedded system remains a mono-

layer, so that each particle interacts with both the bottom and the top plate. The possibility to modify shearons and hence the frictional response by (i) (ambient) pressure and (ii) defects at the plates should be realizable experimentally.

Acknowledgment. Financial support from the Israel Science Foundation, the German Israeli Foundation, and DIP and SISITOMAS grants is gratefully acknowledged. M.P. gratefully acknowledges the Alexander von Humboldt foundation (Feodor Lynen program) for financial support.

References and Notes

(1) Bowden, F. P.; Tabor, D. *The Friction and Lubrications of Solids*; Clarendon Press: Oxford, 1985; Persson, B. N. J. *Sliding Friction, Physical Properties and Applications*; Springer Verlag: Berlin, 1998.

(2) Granick, S. *Physics Today* **1999**, *52*, 26.

(3) Yoshizawa, H.; McGuiggan, P.; Israelachvili, J. *Science* **1993**, *259*, 1305. Hu, H.-W.; Carson, G. A.; Granick, S. *Phys. Rev. Lett.* **1991**, *66*, 2758. Klein, J.; Kumacheva, E. *Science* **1995**, *269*, 816. Berman, A. D.; Drucker, W. A.; Israelachvili, J. *Langmuir* **1996**, *12*, 4559.

(4) Tomlinson, G. A. *Phil. Mag.* **1929**, *7*, 905.

(5) Tompson, P. A.; Robbins, M. O.; Grest, G. S. *Isr. J. Chem.* **1995**, *35*, 93.

(6) Rozman, M. G.; Urbakh, M.; Klafter, J. *Phys. Rev. Lett.* **1996**, *77*, 683.

(7) Carlson, J. M.; Batista, A. A. *Phys. Rev. E* **1996**, *53*, 4253. Batista, A. A.; Carlson, J. M. *Phys. Rev. E* **1998**, *57*, 4986.

(8) Braiman, Y.; Family, F.; Hentschel, H. G. E. *Phys. Rev. E* **1996**, *53*, R3005. *Phys. Rev. B* **1997**, *55*, 5491.

(9) Gao, J. P.; Luedtke, W. D.; Landman, U. *Phys. Rev. Lett.* **1997**, *79*, 705.

(10) Rozman, M. G.; Urbakh, M.; Klafter, J. *Europhys. Lett.* **1997**, *39*, 183. Rozman, M. G.; Urbakh, M.; Klafter, J.; Elmer, F.-J. *J. Phys. Chem. B* **1998**, *102*, 7924. Zaloj, V.; Urbakh, M.; Klafter, J. *Phys. Rev. Lett.* **1998**, *81*, 1227.

(11) Elmer, F.-J. *Phys. Rev. E* **1998**, *57*, R4903.

(12) Baumberger, T.; Caroli, C. *Eur. Phys. J. B* **1998**, *4*, 13.

(13) Sokoloff, J. B. *Phys. Rev. B* **1995**, *51*, 15573. Sokoloff, J. B.; Tomassone, M. S. *Phys. Rev. B* **1998**, *57*, 4888.

(14) Röder, J.; Hammerberg, J. E.; Holian, B. L.; Bishop, A. R. *Phys. Rev. B* **1998**, *57*, 2759.

(15) He, G.; Müser, M. H.; Robbins, M. O. *Science* **1999**, *284*, 1650.

(16) The anharmonic inter-particle potential is defined such that, close to the minima, the resulting force equals the harmonic one.

(17) This definition is also used in the case of periodic boundary conditions, where the center of mass is no more uniquely defined.

(18) Smith, E. D.; Robbins, M. O.; Cieplak, M. *Phys. Rev. B* **1996**, *54*, 8252.

(19) Braiman, Y.; Hentschel, H. G. E.; Family, F.; Mak, C.; Krim, J. *Phys. Rev. E* **1999**, *59*, R4737.

(20) Hentschel, H. G. E.; Family, F.; Braiman, Y. *Phys. Rev. Lett.* **1999**, *83*, 104.

(21) Weiss, M.; Elmer, F.-J. *Z. Phys. B* **1997**, *104*, 55.

(22) Porto, M.; Urbakh, M.; Klafter J. Unpublished.

(23) Porto, M.; Urbakh, M.; Klafter, J. *Europhys. Lett.*, in press.

(24) Yoshizawa, H.; Israelachvili, J. *J. Phys. Chem.* **1993**, *97*, 11300.